ELSEVIER

Agricultural and Forest Meteorology 83 (1997) 27–36

AGRICULTURAL AND FOREST METEOROLOGY

High-resolution snow–water equivalent measurement by gamma-ray spectroscopy

William L. Bland [a,*], Philip A. Helmke [a], John M. Baker [b]

[a] *Department of Soil Science, University of Wisconsin–Madison, 1525 Observatory Drive, Madison, WI 53706, USA*

[b] *US Department of Agriculture, Agricultural Research Service, St. Paul, MN 55108, USA*

Received 19 October 1995; revised 7 March 1996; accepted 28 March 1996

Abstract

Frozen precipitation has important implications for water quality and soil biology. Nutrients in landspread animal manure are transported to surface waters by snowmelt, and winter survival of forages often depends on snow cover. Further development of mechanistic snow behavior models would be assisted by improved measurements of the disappearance of water from snowpacks. We developed a system to measure the total water content (snow-water equivalent, SWE) of a snow cover based on attenuation of γ-rays. A mixed Eu-152, 154 source (about 70 MBq) was pushed through raceways which were placed on the soil surface prior to snowfall. Attenuation of the emitted radiation by solid and liquid water in snow was measured with a Ge detector held above the snow and a multichannel analyzer. Use of four energy peaks and solution of the six resulting equations reduced dependence of the measurement on source–detector geometry. In laboratory tests, measurements of a fixed water depth (30 mm) were constant to ± 1.5 mm following displacement of the detector by 50 mm laterally and 100 mm vertically, a much larger repositioning error than occurs in the field. Field tests showed that the system detected melting conditions with greater sensitivity than was attained with collecting of snow cores. Errors in estimated SWE due to repositioning of the detector were about ± 3 mm. Estimated energy balance terms were in reasonable agreement with observed melting during a field experiment. The new device will allow non-destructive SWE measurements to assess the influences of a number of agricultural management practices on winter hydrology.

* Corresponding author.

PII S0168-1923(96)02351-9

1. Introduction

Detailed studies of winter-time processes in and on the soil often require descriptions of the process of disappearance (ablation) of snow. Computer simulation models are an important tool in this regard. Development and thorough testing of these models depends on measurements of the time-dependent nature of the snow cover and, in particular, its equivalent water depth, or snow-water equivalent (SWE). The snow literature is dominated by studies of relatively deep snowpacks of mountainous regions, motivated by human safety and water supply concerns. Consequently, available means of measuring SWE all have limitations with respect to the thinner snow covers of importance in agricultural (non-mountainous) regions.

The simplest SWE measurement technique is collection and melting of cores of snow (Goodison et al., 1981). This approach is plagued by the difficulty of collecting a core of known dimensions in a snow cover with layers of markedly different densities. When a coring tool encounters an ice lens or layer of relatively high density, layers of snow below may be compacted and the collected volume distorted. Additionally, coring is destructive and not repeatable at a single location, introducing error due to spatial variability into attempts to measure small changes in snow cover such as might occur over timescales of several hours. Finally, the boundary between snow and soil can be difficult to delineate, particularly during spring snowmelt.

In situ weighing devices, such as snow pillows and lysimeters, are used to measure changes in SWE. Snow pillows are fluid-filled bladders of the order of several m^2 in area placed on the soil surface to detect changes in the mass of the overlying snow cover (Goodison et al., 1981). Pillows are relatively simple and inexpensive, and allow continuous unattended operation, but snow on the pillow must be maintained free of contact with its surroundings in order for mass changes to be accurately recorded. Heat exchange between the soil and snow is disrupted, causing error. Snow lysimeters (Granger and Male, 1978) allow partitioning of meltwater between evaporation and drainage. However, contact between the snow and soil is lost and care must be taken to prevent contact between snow on and off the device, as with pillows. Lysimeters are more complex and costly than pillows, limiting the number of possible replications.

Attenuation of radioactivity has frequently been used to measure density profiles and total SWE in deep snowpacks (Goodison et al., 1981; Kattelmann et al., 1983; Wheeler and Huffman, 1984). Systems typically have consisted of two or three metal tubes placed vertically in the soil and projecting above the snowpack. Source and detector were lowered into different tubes and the attenuation of a single energy of γ-ray was determined. The presence of tubes projecting through the snow cover causes altered patterns of snow accumulation and melt, and only a single site can be measured with a costly and complex system. Attenuation of natural radioactivity is also routinely used to make large-scale surveys of SWE (National Operational Hydrologic Remote Sensing Center, NOHRSC, 1992). Data are collected with airplane-mounted detectors, and comparison of counts collected along a flightline before and after snow accumulation allows an estimate of SWE. Spatial resolution and accuracy of the technique is adequate for the hydrological survey needs it was developed to meet, but are inadequate for process studies at the field scale.

We require a high-resolution, non-destructive technique for measuring the disappearance of snow covering agricultural fields. Resolution to 1–2 mm of water equivalent is needed to assess the validity of mechanistic models of snow ablation operating at daily or hourly timescales. Additionally, we must be able to measure and predict ablation of snow that is commingled with animal manure spread over the surface. These constraints nudged us in the direction of radioactive attenuation methods, but with the following additional criteria: the system must be capable of measurement at multiple sites, and it must not involve permanent fixtures that could interfere with the accumulation, evaporation, or melting of snow. We report the results of laboratory and field tests to demonstrate that a system meeting the above criteria is feasible and useful.

2. Materials and methods

We developed and tested a system in which SWE is determined by measuring the attenuation of γ radiation emanating from a manufactured source that is moved in a tube which is left in place at the soil surface. The theory is described first, followed by details of the implementation.

2.1. Governing equations

The attenuation of monochromatic γ-rays by matter is given by:

$$\ln(I_i/I_{0i}) = -\mu_i x \tag{1}$$

where I_{0i} is the measured intensity of γ-rays of energy i at the detector in the absence of the absorber, I_i is the measured intensity of γ-rays when the absorber is present, μ_i is the linear attenuation coefficient for the absorber (mm^{-1}) for γ-rays of energy i, and x is the thickness of the absorber (mm). Application of Eq. (1) requires knowledge of I_{0i}, which is highly dependent on the distance between the source and the detector. For example, in a typical application of the system described below, a 10-mm error in source–detector distance results in a 5-mm error in SWE. It appears unlikely that a system that met our objectives could be designed to reproduce the source–detector separation with adequate precision in the field.

If two energies of γ-rays are available, Eq. (1) can be written for each and the equations solved to yield x:

$$x = \frac{\ln(I_1/I_2) - \ln(I_{01}/I_{02})}{(\mu_2 - \mu_1)} \tag{2}$$

The problem of source–detector separation can be relaxed by writing Eq. (2) for several pairs of available γ-ray energies and iterating on the values of I_{0i} to minimize the standard deviation of the resulting set of x estimates. A nominal value is entered for each I_0, selected from a guess of the source–detector separation, and the solution is

constrained to change these values by no more than ±15%. Solution of this set of equations was done in the spreadsheet Microsoft Excel, using the Solver. [1]

2.2. Radioactive source

To create the radiation source, high purity Eu_2O_3 powder was mixed with epoxy cement and sealed into a 20-mm length of high purity quartz tubing that was then fused at both ends. The tube was then irradiated in the University of Wisconsin–Madison nuclear reactor for 45 min at a neutron flux of 9×10^{12} cm^{-2} s^{-1}. The resulting source was approximately 70 MBq of predominately Eu-152 (152:154 ratio of 21:1), an isotope with a half-life of 13.48 years. Radioactive decay is by β-ray emission with approximately 50 γ-ray energy levels between 122 and 1528 keV (Weast, 1983), and characteristic x-rays near 45 keV. The x-rays and the five most intense γ-rays (122, 245, 344, 779, 1408 keV) are used in our work.

The quartz tube source was secured into a 13- by 13- by 50-mm-long brass carrier, grooved on two sides to provide windows for the γ-rays. The carrier was stored and transported in a lead shield, which also mated to square aluminum tubing of 15-mm id and 1-mm wall thickness. This square tubing served as a raceway for the source, and was placed on the soil surface prior to snowfall. The source was pushed and pulled through the raceway and in and out of the shield by a stiff flat metal tape attached to the carrier. At one end and the middle of the raceway, windows were milled through the upward-facing wall and covered with 1-mm thick polycarbonate plastic. Marks on the metal tape allowed positioning of the source beneath these windows. Raceways 3 m long were fabricated and attached to steel toolboxes. The boxes served to align the raceway with the shield when the source was to be deployed (Fig. 1).

2.3. Detector and analyzer

Gamma-rays were counted using a Canberra Industries, Inc. (Meridian, CT) model GC1019 Coaxial Ge detector, a model 2002CSL preamplifier, and a Portable Plus 1150 battery-powered multi-channel analyzer. The detector was cooled with liquid N during operation from an attached 2-l cryostat (system cost about $18000). A notebook computer served as the user interface for the analyzer. At the end of each measurement we recorded net counts in regions of interest defined around the six energy peaks selected for study.

The detector was held 0.1 to 0.6 m above the raceway window at which the source was positioned during measurements. In the current design, the detector is held in position by a 3-m-long triangular tower section mounted horizontally atop a 2-m-tall steel post driven into the ground. The detector is mounted facing downward at one end of the horizontal section. By rotating the tower section on the post the detector can be positioned over either of the two windows in the raceway (Fig. 1).

[1] Mention of a company and/or product does not imply endorsement by the University of Wisconsin–Madison.

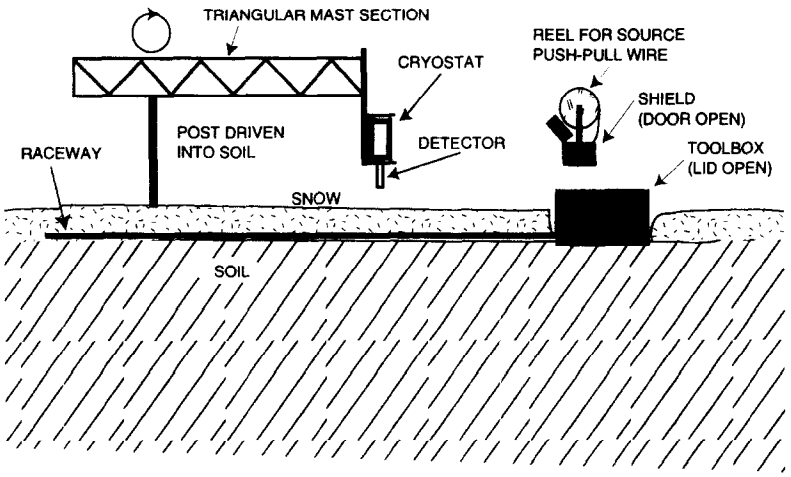

Fig. 1. Side view of the system in the field. The raceway, toolbox, post, and mast section are installed prior to snowfall. To make a measurement, the mast is rotated away from the raceway and the detector/cryostat mounted at the mast end. The mast is then rotated so as to position the detector over one of the windows in the upper face of the raceway. The toolbox is opened and the shield (with door open) is placed in it and slid toward the raceway until the shield and raceway mate. The source is pushed out of the shield and through the raceway by the push–pull wire on the reel attached to the shield, and advanced to the window above which the detector is positioned. The multichannel analyzer which records the counts is housed in a heated vehicle, and is attached to the detector via a 30-m long cable.

2.4. Laboratory and field tests

Three tests of the system were conducted. In a laboratory test to evaluate the effects of source–detector geometry, the detector was initially placed directly above the source at a distance of 0.5 m, with approximately 17 mm of water and 11 mm of polyacrylate plastic intervening. Several vertical and lateral displacements of the detector were then made, with counts recorded for 30 min at each position.

Two field trials were conducted. In 1994, the detector was left in one place during each of 3 days, to evaluate uncertainty in SWE for reasons other than repositioning effects. This trial was conducted on a fall chisel-plowed corn field with a relatively rough surface (soil height differences to 0.3 m within a 1 m distance). The detector was held above the source and raceway by a 3-m-long section of triangular tower held at both ends by posts driven into the soil. The second field trial was conducted in 1995 in an alfalfa field that had been harvested in the fall of 1994; this field was relatively smooth and covered with 0.1-m-tall alfalfa stems.

During 2 days of the 1995 field experiments, other components of the snow energy balance were estimated or measured. Measured parameters were net radiation (Type S-1 Swissteco, Oberrient, Switzerland), soil heat flux (REBS, Seattle, WA), and soil temperature. Two heat flux plates were installed at 10 mm depth prior to soil freezing, as were duplicate thermocouples at 10, 50, and 100 mm. Sensible and latent heat fluxes were estimated using data from a nearby automated weather station and equations given by Campbell (Campbell, 1977). The roughness length for momentum, z_0, over snow

Table 1
Relative count rates of the x- and γ-rays selected for use in the system

	Energy (keV)					
x	45	122	245	344	779	1408
γ	0.32	1.00	0.16	0.42	0.09	0.08

was taken as 3 mm (Morris, 1989), and roughness coefficients for heat and water vapor were assigned the same value. Snow surface temperature was assumed to be 0°C, since melting was occurring.

3. Results and discussion

3.1. Detector calibration

The relative count rates of the six energies of x- and γ-rays chosen for use are shown in Table 1. These values were determined experimentally; they represent the product of the relative intensity of the energy peak and the efficiency of the detector at that energy. A sample calibration of the system to determine μ_i (in Eq. (1) and Eq. (2)) at each energy is shown in Fig. 2. As predicted by Eq. (1), the relationship between $\ln(I/I_0)$ and x is linear. The intercept of each line is $\ln(I_0)$. However, I_0 is an inverse square function of distance between the source and detector. Because this distance cannot be reproduced exactly in the field, Eq. (1) cannot be used for routine measurements and the solution using Eq. (2) is required.

3.2. Sensitivity to source–detector geometry

In order for the system to be useful, the solution provided by Eq. (2) must yield the correct answer for water thickness through a range of relative source and detector

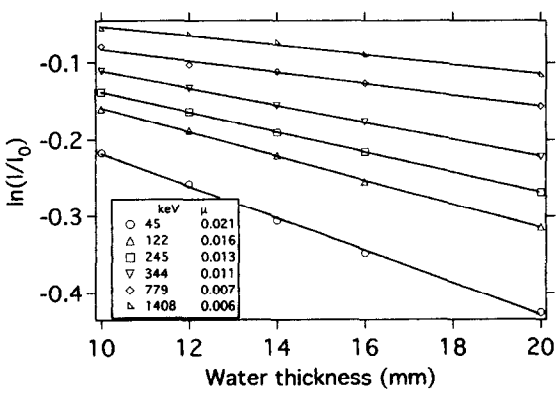

Fig. 2. Calibration of the system to obtain linear extinction coefficients for the six energies of x- and γ-rays used. The source is approximately 70 MBq of Eu-152.

Table 2
Equivalent water depth in a laboratory test, at different relative spatial positions of the source and detector

	Detector 0.5 m directly above source	$\Delta z^a = 0$ mm, $\Delta y = 50$ mm	$\Delta z = -105$ mm, $\Delta y = 50$ mm	$\Delta z = -105$ mm, $\Delta y = 0$ mm
Equivalent water depth (mm)	28.9	29.3	31.5	28.2

[a]Δz is vertical displacement of detector from original position (second column); Δy is lateral displacement of detector from original position.

positions comparable to the variation in placement that might occur in the field. Results of the laboratory test to evaluate this are shown in Table 2. For each detector position relative to the source, estimated equivalent water depth is reported. At the maximum displacement of the detector from its initial location (about 112 mm), estimated water depth (attenuation due to both water and plastic box) changed 2.6 mm, or less than 10%. This displacement is perhaps twice the maximum uncertainty in repositioning that we anticipate should occur in the field. Thus, the proposed solution of Eq. (2) for several energy pairs greatly reduced the need for precise repositioning of the source and detector relative to the requirements imposed by Eq. (1).

3.3. Field experiments

3.3.1. Single position

Snow-water equivalent was measured during 3 days (March 1, 2, and 3) of melt or near-melt conditions, during which the detector was not moved in relation to the source on each day (Fig. 3). The system was removed each night and repositioned the next day (with possible errors of 1–2 mm SWE). On all 3 days air temperatures reached 0°C and skies were generally sunny.

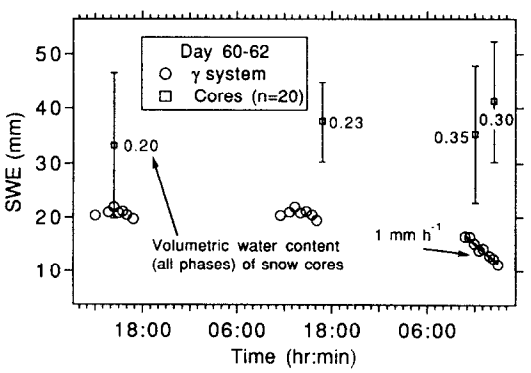

Fig. 3. Results of 3 days of SWE (snow water equivalent, mm) measurements at the start of melting. Snow cores collected at four times did not indicate decreasing SWE during the period, but did show an increase in volumetric water (all phases) content of the snow; error bars are SD of 20 cores sampled. The γ system measurements substantiated visual assessments of melting on the third day. Noise in the γ system SWE estimate was on the order of 1 mm, judging from the results of days of year 60 and 61.

Snow cores ($n = 20$) gathered once-daily for the first 2 days and twice on the third day demonstrated the large variability that is typical of this method of estimating SWE (Fig. 3). It is unclear how much of this variability is due to measurement error and how much is due to true variation in snow cover, but regardless of the apportionment we can conclude that measurement of the rate of snowpack ablation using gravimetry will have extremely coarse temporal (or depth) resolution. On the other hand, γ attenuation appears to afford depth resolution on the order of 1 mm, which should be sufficient for many applications. Values of SWE measured by the γ system showed decreases only on the third day, at a rate of 1 mm h^{-1}. This agreed with visual assessments based on runoff, although infiltration, if it were occurring, would not be detected visually. Snow core data could not have quantified this melting at the precision possible with the γ system (Fig. 3). The site of the γ system measurement had less snow cover than did the majority of the cored sites. This is likely, because we installed the raceway tubes nearer to high points of the chisel-plowed soil surface than to low points. To the extent that the gravimetric data indicate true spatial variation, we conclude that the γ system must be capable of measuring at a number of sites in a field to yield a reasonable estimate of areally averaged SWE.

3.3.2. Repositioning tests

Fundamental to measuring changes in the areal average SWE is the ability to move the γ system among a number of measurement sites. This ability was tested on a day (day of year 48) during which the source and detector were moved among several locations (alternating between windows in a raceway, and between two raceways in the same field). During the day the snow consolidated appreciably, although extensive melting was not apparent, nor was runoff observed (Fig. 4). Assuming negligible change in SWE during the period, uncertainty in the measurement appears to be approximately 2–3 mm. Some of this may have been due to wind-driven movement of the detector. Even after stabilization of the mast supporting the detector with shock cords, back-and-forth movements spanning at least 50 mm were observed. (A new design holds the detector in the center of a four-legged aluminum framework, eliminating wind effects.)

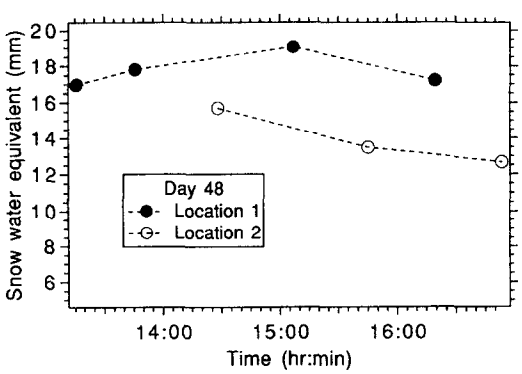

Fig. 4. Measurements SWE (snow water equivalent, mm) prior to water loss from the snowcover, during which the γ system was moved between two sites. Errors in SWE due to repositioning were perhaps as high as 3 mm, possibly due to wind-driven movement of the detector.

3.3.3. Interpretation of SWE measurements in conjunction with energy balance estimates

On Day 49, net radiation and soil heat flux were measured, and latent and sensible heat fluxes were calculated, while SWE measurements were made with the γ system. Additionally, this was a day during which rapid melting and subsequent disappearance of the snowpack occurred. Fig. 5(A) shows the energy balance measurements and estimates, while Fig. 5(B) contains the SWE measurements. These were made a three different locations in the field and at each two or more measurements were made.

The first SWE value measured at Location 1 (Fig. 5(B)) on Day 49 was 13 mm, compared to about 17 mm at the same position at the end of the previous day (Fig. 4). This difference is similar to the 2–3 mm uncertainty described in the previous section, and some drainage from the snow may have occurred after the previous day's measurement. While water likely was condensing on the snowpack during late morning and the afternoon of Day 49, the rate was much smaller than that indicated by the second measurement at Location 1. It is not uncommon for condensation to contribute to the melt process (McKay and Thurtell, 1978) when warm, relatively moist air masses move over snow cover, where surface temperature and vapor pressure cannot exceed 0°C and 0.67 kPa. Later in the day, the SWE measurements showed net decreases as the melt process progressed, and runoff became visually apparent at the field edge. Integration of

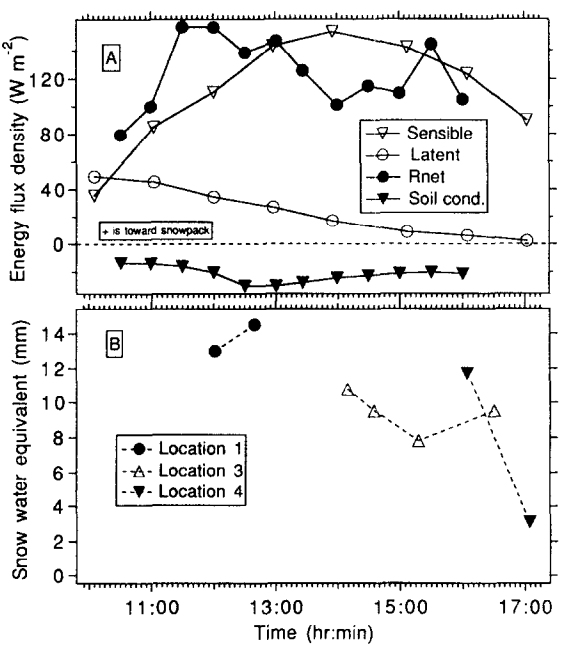

Fig. 5. (A) Energy budget terms during the afternoon of day of year 49. Net radiation and soil heat conduction were measured near the SWE measurement site (later data not available). Latent and sensible heat fluxes were estimated from measurements made at a nearby automated weather station. (B) Measurements of SWE (snow water equivalent, mm) at three locations during the same time period as shown in (A). Location 1 corresponds to the same location in Fig. 4. A flux divergence to the snow of about 4 MJ m^{-2} was estimated for the period 12.00 to 17.00 h, and the observed outflow of 9 mm SWE required 3 MJ m^{-2} day^{-1} to melt.

the energy fluxes (Fig. 5(A)) from 12.00 to 17.00 h resulted in a net input to the snow of about 4 MJ m^{-2}. It was not until 13.30 h that the 10-mm soil temperature rose above -0.1°C, so prior to this, the energy flux warmed and melted snow. Assuming SWE at 12.00 h was about 12 mm, a total of 9 mm was observed to drain from the snowpack by 17.00 h, mostly from 16.00 to 17.00 h. Melting of this 9 mm of water required 3 MJ m^{-2}, close to the 4 MJ m^{-2} estimated to have been supplied to the snow. The snow cover was essentially gone (SWE about 2 mm) at this point. While there is much uncertainty in this calculation, particularly related to the turbulent flux estimates, it demonstrates that the SWE measurement appears reasonable with respect to the overall energy balance.

4. Conclusions

We conclude that the γ system has sufficient resolution to measure changes in SWE associated with snowmelt on a sub-daily timescale. Use of a multichannel analyzer and Eq. (2) with several pairs of γ-ray energies relaxes the need for exact reproduction of source–detector placement, enabling relatively precise measurements of SWE at several locations in a field. However, field results show that improvements should be made in the apparatus and methodology to allow measurements at a larger number of sites than is currently possible, in order to adequately represent variability in snow cover. The system should be a valuable tool in assessing the effects of cultural practices, such as manure application and fall tillage, on the hydrology of spring snowmelt in agricultural fields.

References

Campbell, G.S., 1977. An Introduction to Environmental Biophysics. Springer-Verlag, NY, 159 pp.

Goodison, B.E., Ferguson, H.L. and McKay, G.A., 1981. Measurement and data analysis. In: D.M. Gray and D.H. Male (Editors), The Handbook of Snow. Pergamon, New York, pp. 191–273.

Granger, R.J. and Male, D.H., 1978. Melting of a prairie snowpack. J. Appl. Meteorol., 17: 1833–1842.

Kattelmann, R.C., McGurk, B.J., Berg, N.H., Bergman, J.A., Baldwin, J.A. and Hannaford, M.A., 1983. The isotope profiling snow gage: Twenty years of experience. In: Proc. 51st Annual Meeting Western Snow Conference, 19–21 April 1983, Vancouver, WA. pp. 1–8

McKay, D.C. and Thurtell, G.W., 1978. Measurements of the energy fluxes involved in the energy budget of a snow cover. J. Appl. Meteorol., 17: 339–349.

Morris, E.M., 1989. Turbulent transport over snow and ice. J. Hydrol., 105: 205–223.

National Operational Hydrologic Remote Sensing Center (NOHRSC), 1992. Airborne Gamma Radiation Snow Survey Program and Satellite Hydrology Program User's Guide, v. 4.0. National Operational Hydrologic Remote Sensing Center, Minneapolis, MN.

Weast, R.C. (Editor), 1983. CRC Handbook of Chemistry and Physics. 63rd edn., CRC Press, Boca Raton, FL, 1981 pp.

Wheeler, P.A. and Huffman, D.J., 1984. Evaluation of the isotopic snow measurement gage. In: Proc. 52st Annual Meeting Western Snow Conference, 17–19 April 1984, Sun Valley, ID. pp. 48–52.